Hybrid Features for Face Recognition

(IJCSNT) International Journal of
Communication Systems and Network
Technologies
ISSN Number: 2053-6283
Volume 1, Issue No. 2, 116–126

https://journals.mirlabs.in/index.php/ijcsnt
DOI: 10.18486/ijcsnt/1.2.010
IJCSNT

M. Hanmandlu[1], Farrukh Sayeed[2], A. Q. Ansari[3]

Abstract

This paper explores the combination of two types of features to evolve hybrid features. The first hybrid features arise on the application of the fuzzification function on the wavelet decomposed images and the second hybrid features are the result of applying the fuzzification function on the convolved face images with the Gabor filter bank. The Gabor fuzzy features show a better performance in terms of ROC whereas the wavelet fuzzy features have an edge over the Gabor fuzzy features in terms of identification accuracy as given by support vector machines (SVM). The algorithm was tested on ORL (Olivetti Research Laboratory) database that has slight orientations in face images.

Keywords

Gabor Filter Bank, Haar Wavelets, Muti-decomposition, Wavelet-fuzzy Features, Gabor Fuzzy Features, SVM.

Received: 12 May 2012; **Revised:** 19 July 2012; **Accepted:** 18 August 2012;
Published: 30 August 2012;

[1]E.E Department, I.I.T., New Delhi, India.
[2]E&C. Department, P.A. College of Engineering, Mangalore, Karnataka, India.
[3]E.E Department, JMI, New Delhi, India.

Corresponding author:
Email: mhmandlu@gmail.com

Introduction

The face recognition is one of the most important applications of the Biometric based authentication systems. During the past few decades, it has received a considerable attention, because of a large number of application areas such as Entertainment, Smart Cards, Information Security, Law Enforcement, Surveillance etc.

Face recognition involves a range of activities from many aspects of human life. Humans are good at face recognition and now machine learning is being improved to do this task. Identification of people in different environments requires three steps: acquisition, normalization and recognition. Acquisition involves the detection and tracking of face-like patches in the dynamic scenes. Normalization is the segmentation, alignment and standardization of the face images, and finally recognition is concerned with the representation via modeling of face images and association of face images with the models learned.

The methods reported in the literature are broadly classified into: i) Holistic matching methods in which the whole face acts as an input to the recognition system, ii) Feature based matching methods, in which as the name indicates, the local features such as eyes, mouth, and nose are first extracted and their locations and the local statistics are fed to the recognition system, and iii) Hybrid methods where the recognition system makes use of both the local features as well as the whole face region to recognize the face.

Schneiderman and Kanade[8] apply statistical likelihood tests using feature output histograms to create the detection scheme. Rowley and Kanade in[7] use neural network-based filters to obtain the benchmark results. In another early work, Papageorgiou et al.[5] propose a general object detection scheme that uses a wavelet representation and statistical learning techniques. Osuna et al.[4] apply Vapnik's support vector machine for the face detection, and Romdhani et al.[6] improve upon this work by creating the reduced training vector sets. Fleuret and Geman attempt a coarse-to-fine approach to face detection, focusing on minimizing the computation involved[3]. In perhaps the most impressive paper, Viola and Jones use the concept of an "integral image", along with the rectangular feature representation and Adaboost learning algorithm to detect faces at the rate of 15 frames per second[2]. Several basic face recognition techniques exist suitable to the frontal faces. These include: eigenfaces, neural networks, dynamic link architecture, hidden Markov model and geometrical feature matching. These approaches are analyzed in terms of the facial representations adopted by them[1].

The Proposed Hybrid Features

Here we will be exploring two hybrid features, viz., Wavelet-fuzzy and Gabor-fuzzy. We will now elaborate these features.

Wavelet Fuzzy Features

Wavelets are immensely suitable for texture analysis. We are inclined to investigate the effectiveness of Haar wavelets on the face. Simplicity of these wavelets is an overriding factor in the choice of these wavelets though other celebrated wavelets such as Daubechies wavelets, Symlets are also tried but the improvement accrued from the latter ones does not justify their use[9].

A two-dimensional discrete wavelet transform is applied on the ROI of a face resulting in four subbands: HL1, LH1 and HH1 which correspond to detail images, viz., Horizontal H_1, Vertical V_1, and Diagonal D_1 respectively, and LL1 which corresponds to Approximation image A_1 at the first level of decomposition. Note that H_1, V_1 and D_1 together contribute to a detail image. Thus in any decomposition, the detail images include horizontal, vertical and diagonal parts. The subscript 1 changes to i for the ith level of decomposition. Fig. 1 shows one level of decomposition. Note that A1 can be further decomposed into four sub bands and the process is repeated till the information from An at the nth decomposition is insignificant.

In this work, a face image is decomposed into three time scales using Haar wavelets. At the third level of decomposition the approximation image A3 is very insignificant hence it is not considered. But the detail images in all three decompositions are considered for feature extraction. The three detail images (H_i, V_i, D_i) resulting from decomposition are superimposed to yield a Composite image Si. It may be noted that as the decomposition level increases the size of the detail images also decreases.

As we have three decompositions there will be three composite detail images Sd, d=1,2,3 of different sizes (i.e. the size of 1st Composite detail image S_1 is 56x46; that of 2nd composite detail image S_2 is 28x23 and of 3rd Composite detail image S_3 is 14x12). These images are divided into non overlapping windows of size WxW[10]. The total number of windows k=1,2,...,K is dependent upon the size of the window chosen. From each window, energy feature is calculated as:

$$S_d(x, y) = H_d(x, y) + V_d(x, y) + D_d(x, y), \quad d = 1, 2, 3 \tag{1}$$

$$E_d(k) = \sum_{x=1}^{W} \sum_{y=1}^{W} (S_d(x, y))^2, \quad d = 1, 2, 3 \tag{2}$$

where k is the k^{th} window in d^{th} Composite detail image. Note that the three windows K from three Composite detail images provide us the features. However, the Composite detail images are not utilized for the extraction of features because the Approximation images are found to yield better performance.

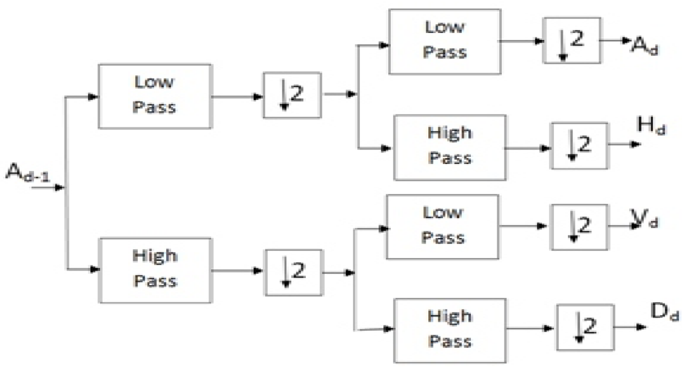

Figure 1. 2D one-level DWT decomposition

The faces generally possess random texture. We are mainly interested in capturing the random texture from the Approximation images Ai. We will now see how to tap the uncertainty from the Approximation images arising out of the decompositions discussed above. As we have three decompositions there are three Approximation images. As noted above the third Approximation image is quite insignificant so we are left with two Approximation images A1 and A2 for extracting the fuzzy features.

These Approximation images separately become ROI's for the extraction of fuzzy features. The steps involved in this process are explained in the following algorithm.

An algorithm for the feature extraction

1. The ROI is divided into a number of non-overlapping windows of size WxW.
2. The average intensity Iavg in the k^{th} window is found using:

$$I_{avg}(k) = \frac{1}{WxW}\sum_{x=1}^{W}\sum_{y=1}^{W} I(x,y) \tag{3}$$

3. The maximum intensity, I_{max} in the k^{th} window is found.
4. The membership function μ_{xy} of every pixel in the k^{th} window is computed from

$$\mu_{xy} = \left(\frac{|I(x,y) - I_{avg}(k)|}{I_{max}}\right) \tag{4}$$

The above membership grade gives very low values(0 to 0.2); so we subtract it from unity to make them close to 1 in the range (0.8 to 1). In view of this we consider as the membership function. Note that the membership function in (4) has an arbitrary shape but captures the random texture quite effectively.

5. The cumulative response representing the texture information in the k^{th} window is computed from:

$$I_{\bar{\mu}}(k) = \frac{\sum\sum(\bar{\mu}_{xy} \cdot I(x,y))}{\sum\sum\bar{\mu}_{xy}} \tag{5}$$

The above cumulative response represents the texture. It is called a fuzzy feature for it is derived using fuzzy logic.

Note that the fuzzy features are the outcome of the fuzzification of the Approximation images.

As far as the extraction of wavelet-fuzzy features is concerned, four windows of sizes 3x3, 5x5, 7x7 and 9x9 are taken for the experimentation. The lengths of wavelet-fuzzy feature vectors corresponding to four windows come out to 270; 99; 48; 30 on A1 and 63; 20; 12; 06 on A2. These features are subject to classification by both Euclidean distance and SVM classifiers.

Gabor Fuzzy Features

Here we use the Gabor filter bank with different orientations and frequencies. The output of each filter is convolved with the original image I(x,y) and the convolved outputs of the different filters are averaged to get the features of the image. A set of Gabor functions is used to extract features from face images. The filter function has two parts given by

$$f(x,y) = f^r(x,y) + jf^i(x,y) \tag{6}$$

Where $f^r(x,y)$ and $f^i(x,y)$ are the real and imaginary parts of 2D Gabor filters respectively. They have the following forms:

$$f^r(x,y) = \frac{1}{2\pi\lambda\gamma}\exp\left[-\frac{1}{2}\left(\frac{x'^2}{\lambda^2}+\frac{y'^2}{\gamma^2}\right)\right]\cos(2\pi F_u x') \tag{7}$$

$$f^i(x,y) = \frac{1}{2\pi\lambda\gamma}\exp\left[-\frac{1}{2}\left(\frac{x'^2}{\lambda^2}+\frac{y'^2}{\gamma^2}\right)\right]\sin(2\pi F_u x') \tag{8}$$

Where,

$$x' = x\cos(\theta_v) + y\sin(\theta_v)$$
$$y' = -x\sin(\theta_v) + y\cos(\theta_v)$$

F_u is the frequency of the sinusoidal plane wave, θ_v is the orientation of Gabor filter, λ and γ are the standard deviations of Gaussian envelope along x and y directions respectively. These are considered as scales. In this study we fix both λ and γ to 3 though these can also be varied accruing another leverage to manipulate the Gabor filter.

In Eqs.(7) and (8), frequency F_u and orientation are defined by $F_u = F_{max}/2^{(u/2)}$, $u = 1, 2, 3$ and $\theta_v = \frac{v\pi}{4}$, respectively. We take $F_{max} = 0.25$ in our experiments. Each filter function f(x,y) is convolved with the original image with coordinates x and y, $\{I(x,y)\}$ to get the complex Gabor output $E_{u,v}(x,y)$ as

$$E_{u,v}(x,y) = I(x,y) * f(x,y) \tag{9}$$

This complex output can be decomposed into the real and the imaginary components as

$$R_{u,v}(x,y) = \mathrm{Re}[E_{u,v}(x,y)] \tag{10}$$

$$I_{u,v}(x,y) = \mathrm{Im}[E_{u,v}(x,y)] \tag{11}$$

Using the above, magnitude component $M_{u,v}(x,y)$ and phase component $P_{u,v}(x,y)$ are computed from

$$M_{u,v}(x,y) = \sqrt{R^2_{u,v}(x,y) + I^2_{u,v}(x,y)} \tag{12}$$

$$P_{u,v}(x,y) = \tan^{-1}\left(\frac{I_{u,v}(x,y)}{R_{u,v}(x,y)}\right) \tag{13}$$

We will now consider only the magnitude component as it varies significantly with the spatial position of the Image whereas the phase component is neglected as it varies randomly.

There are 12 Gabor filters corresponding to 3 frequencies and 4 orientations that we have taken for the filter bank. After convolution with a face image, we get 12 magnitude images. These are averaged out to get a composite magnitude image of size 112x92. This is resized into the desired image of size 32x32, which yields the feature vector of length 32x32 = 1024.

All the outputs of the Gabor filter bank called Gabor images (12 Gabor filters with 3 frequencies and 4 orientations) are aggregated and forms the ROI

An algorithm for the feature extraction:

1. The ROI is divided into a number of non-overlapping windows of size WxW.

2. The average intensity Iavg in the k^{th} window is found using (3)
3. The maximum intensity, Imax in the k^{th} window is found.
4. The membership function μ_{xy} of every pixel in the k^{th} window is computed from (4).

In this case also, the above membership grade gives very low values(0 to 0.2); so we subtract it from unity to make them close to 1 in the range (0.8 to 1). In view of this we consider as the membership function.

5. The cumulative response representing the texture information in the k^{th} window is computed using Eq.(5)

Thus Gabor fuzzy features are extracted from the aggregated Gabor image for different window sizes (3x3,5x5,7x7,9x9)

Results of Implementation

The performance of hybrid features is judged on the ORL database which consists of 40 users and 10 sample faces per user. We have two classifiers: Euclidean distance and SVM. The results of application of SVM on wavelet-fuzzy features and Gabor-fuzzy features are shown in Tables 1,2, 3 and 4 respectively. Here we have considered two training to test sample ratios 6:4 and 7:3 for each user.

The implementation of hybrid features on face images is now discussed. A sample face from the database is shown in Fig.2. The twelve magnitude images obtained from the original face with the application of Gabor filter bank of 12 filters are shown in Fig. 3. The 12 magnitude images are aggregated into a composite magnitude image. The size of this image, 112x92 is reduced to 32x32 and the features called Gabor-fuzzy are extracted. Application of SVM on these gives the maximum recognition rate of 96.8% with the kernel of degrees 3 on window size of 9x9 on 6:4 training test sample ratio. However, the performance improves to 97.5% on the same window size but with the kernel of degree 3 and the training to test sample ratio of 7:3. The performance of SVM on wavelet fuzzy features with the window sizes of 5x5 and 7x7 at the decomposition level of 1 with the training to test sample ratio of 6:4 is 96.8%. However the performance of SVM on wavelet-fuzzy features shoots up to 97.5% on a window size of 3x3 at the decomposition level of 2. The performance of wavelet fuzzy features with SVM yields the accuracy rate of 97.5% on the window size of 3x3 using the three kernels of degrees 1,2 and 3 for the decomposition level of 2 and the training to test sample ratio of 7:3. As SVM gives only the classification (recognition) accuracy, it does not provide the error rates required for plotting ROC. In this context, Euclidean distance classifier eliminates this shortcoming. The ROCs resulting from the application of Euclidean classifier on the two hybrid features (wavelet-fuzzy and Gabor-fuzzy features) are shown in Figs. 4-5. With wavelet fuzzy features we get GAR of 87.5% at FAR of 0.1 on the window size of 7x7 at the first decomposition level and GAR of 85.9% at FAR of 0.1 on the window size of 3x3 at the second decomposition level. With Gabor fuzzy features we also get GAR of 87.5% at 0.1 FAR on the window size of 3x3.

A comparison: To see the relative performance of wavelet-fuzzy and Gabor-fuzzy features, the wavelets and Gabor filter bank are separately applied. The wavelets give GAR of 86.25% on the second Approximation images with SVM for the training to test sample ratio of 6:4 (Table 5) whereas Gabor filter gives 96.2% on the same ratio (Table 6).

The ROC of wavelets show GAR of 65% at FAR of 0.1 on Approximation images in Fig. 6 and that of Gabor filter shows GAR of 81.5% at FAR of 0.1 in Fig. 7. It may be observed that there is considerable improvement wavelet-fuzzy features whereas the improvement is marginal with Gabor-fuzzy features.

Table 1. Results of SVM on Wavelet-Fuzzy features on Approximation Images (6 training: 4 test images)

	Level 1				Level 2			
Degree	3x3	5x5	7x7	9x9	3x3	5x5	7x7	9x9
1	95.6	96.2	96.8	96.2	96.8	93.1	93.1	69.3
2	96.2	96.8	96.2	95	97.5	91.8	93.1	70
3	96.2	96.8	96.2	93.7	96.8	92.5	91.8	70.6

Table 2. Results of SVM on Wavelet-Fuzzy features on Approximation images (7 training: 3 test images)

	A1				A2			
	3x3	5x5	7x7	9x9	3x3	5x5	7x7	9x9
1 degree	95.8	95.8	95.8	95.8	97.5	94.1	93.3	71.6
2 degree	95.8	96.6	96.6	95.8	97.5	94.1	93.3	75
3 degree	95.8	96.6	96.6	95.8	97.5	94.1	90.8	75.8

Table 3. Results of SVM on Gabor-Fuzzy features

Training: test	6 training: 4 test			
Window	3x3	5x5	7x7	9x9
1 degree	95.6	95.6	95.6	95.6
2 degree	96.2	96.2	96.2	96.2
3 degree	96.2	96.2	96.2	96.8

Table 4. Results of SVM on Gabor-Fuzzy features

Training: test	7 training: 3 test			
Window	3x3	5x5	7x7	9x9
1 degree	95.8	95.8	95.8	95.8
2 degree	95.8	95.8	95.8	95.8
3 degree	95.8	95.8	96.6	97.5

Figure 2. The original Image

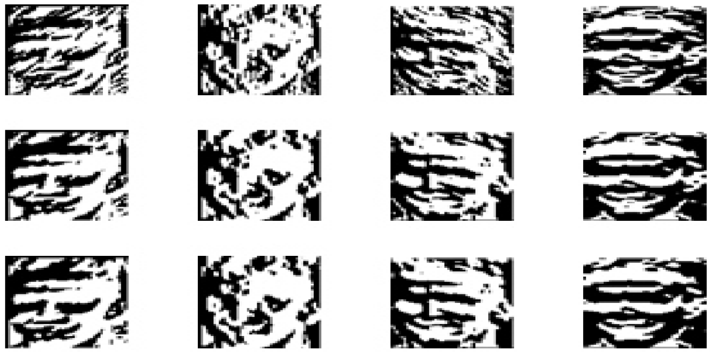

Figure 3. Twelve Magnitude images for the face image

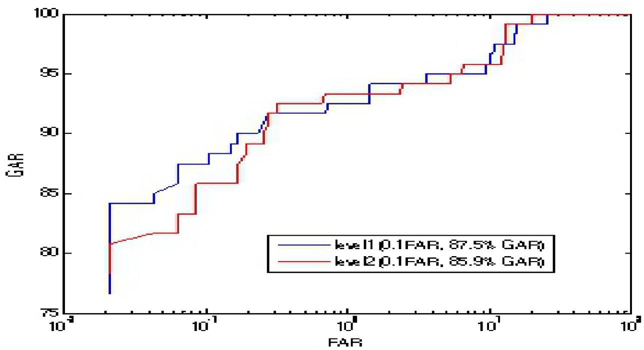

Figure 4. ROC of wavelet-fuzzy features from two Approximation images on the window sizes of 7x7, 3x3.

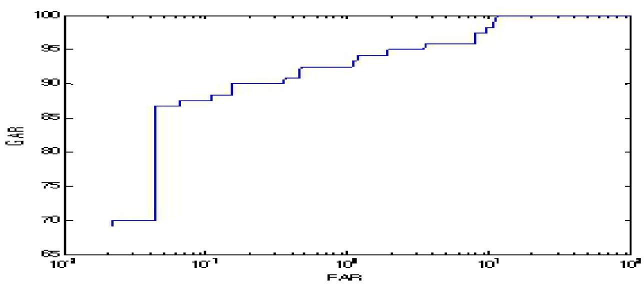

Figure 5. ROC of Gabor-fuzzy features (GAR of 87.5% at 0.1 FAR)

Table 5. Results of SVM on Wavelet features (approximation Images) for the training to test sample ratio of 6:4

	Level 1		Level 2		Level 3	
Degree	3x3	5x5	3x3	5x5	3x3	5x5
1	81.25	84.37	85.62	86.25	85.62	86.17
2	74.37	78.75	78.75	85.62	78.75	85.62
3	63.12	70	70.62	82.5	70.62	83.12

Table 6. Results of SVM with Gabor features

Different kernels	Recognition rate with 6 training + 4 testing
Linear	95.85
2 degree	96.25
3 degree	96.25

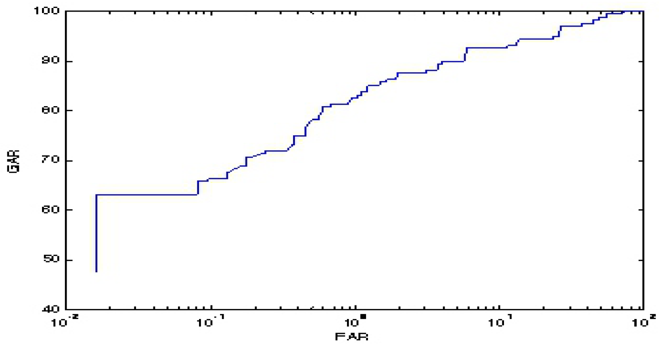

Figure 6. ROC with wavelet features

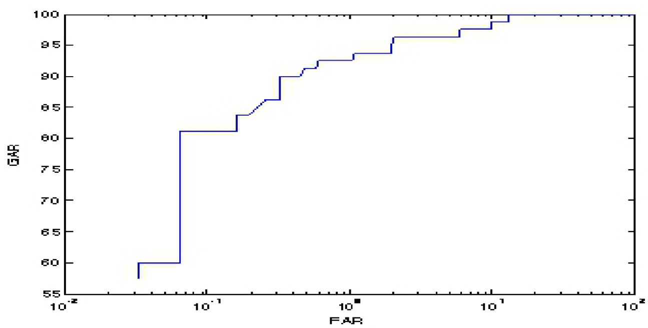

Figure 7. ROC with Gabor features

Conclusions

Two hybrid features, viz., wavelet-fuzzy and Gabor-fuzzy are investigated in this paper. The wavelet-fuzzy features are the result of extracting fuzzy features from two Approximation images. These features are tested using SVM classifier for the training to test sample ratios of 6:4 and 7:3. The recognition has attained the recognition rate of 97.5% on the window size of 3x3 at the second level of decomposition with both ratios. The results of wavelets-fuzzy features on composite detail images are not given here for they are inferior.

The Gabor fuzzy features using SVM classifier yield somewhat inferior recognition rate of 96.8% on the training to test ratio of 6:4. The same Gabor fuzzy features give 97.5% for the training to test ratio of 7:3 on the window size of 9x9 with kernel of degree 3. Thus both hybrid features have the same performance but computationally wavelets are much simpler.

In terms of ROC, wavelet fuzzy features depict GAR of 87.5% at FAR of 0.1 on the window size of 7x7 at the first decomposition level and Gabor fuzzy features also have the same GAR but on the window size of 3x3.

An appraisal of the performance of the two hybrid features on two classifiers indicates that SVM is better suited to classification over Euclidean distance. As far as the recognition rate is concerned, the Gabor-fuzzy features are found comparable to the wavelet fuzzy features.

References

[1] Peng Yao, Jun Li, Xueyi Ye, Zhenquan Zhuang, Bin Li, "Iris Recognition Algorithm Using Modified Log-Gabor Filters," 18th International Conference on Pattern Recognition (ICPR'06) 20–24 August, 2006, Hong Kong, Vol. 4, pp 461–464.

[2] Paul Viola and Michael Jones, "Robust real-time face detection", International Journal of Computer Vision, Vol. 57, Issue 2, pp 137–154, May 2004.

[3] Francois Fleuret and Donald Geman, "Coarse-to-fine face detection", International Journal of Computer Vision, Vol. 41, Issue 1–2, pp. 85–107, Jan-Feb, 2001.

[4] E. Osuna, R. Freund, and F. Girosi, "Training Support Vector Machines: An application to Face Detection", IEEE Computer Society Conference on Computer Vision and Pattern Recognition, 17–19 June, 1997, Puerto Rico, pp 130–136.

[5] C. P. Papageorgiou, M. Oren, and T. Poggio, "A General Framework for Object Detection", Proceedings of Sixth International Conference on Computer Vision, 4–7 January 1998, Bombay, India, pp. 555–562.

[6] S. Romdhani, P. Torr, B. Scholkopf, and A. Blake, "Computationally Efficient Face Detection", 8th IEEE International Conf. on Computer Vision, 07–14 July, 2001, Vancouver B.C., Canada, Vol. 2, pp 695–700.

[7] Henry A. Rowley, Shumeet Baluja, and Takeo Kanade, "Neural Network-Based Face Detection", IEEE Transactions on Pattern Analysis and Machine Intelligence, Vol. 20, Issue No. 1, pp 23–38, January 1998.

[8] H. Schneiderman and T. Kanade, "A Statistical Approach to 3D Object Detection Applied to Faces and Cars", IEEE Conference on Computer Vision and Pattern Recognition, South Carolina 13–15 June 2000, Vol. 1, pp 746–751.

[9] Vitomir Struc, R Gajsek, Nilola Pavasic, "Principal Gabor Filters for Face Recognition", 3rd IEEE International Conference on Biometrics: Theory, Applications and Systems, 28–30 September 2009, Washington DC, pp 1–6.

[10] Xiang-Qian Wu, and Kuan Quan Wang, David Zhang, "Wavelet Based Palmprint Recognition", First International Conference on Machine learning and Cybernetics, 4–5 November, 2002, Beijing, pp 1253–1257.